



# Oxidative dehydrogenation of ethane over vanadium-based hexagonal mesoporous silica catalysts

L. Čapek<sup>\*</sup>, R. Bulánek, J. Adam, L. Smoláková, H. Sheng-Yang, P. Čičmanec

University of Pardubice, Faculty of Chemical Technology, Department of Physical Chemistry, Nam. Cs. Legii 565, CZ-532 10 Pardubice, Czech Republic

## ARTICLE INFO

### Article history:

Available online 5 August 2008

### Keywords:

ODH  
Ethane  
Hexagonal mesoporous silica  
Active species

## ABSTRACT

Vanadium-containing hexagonal mesoporous silica catalysts were tested in oxidative dehydrogenation of ethane. V-HMS catalysts (0.3–9.0 wt.% V) were prepared by impregnation with solution of vanadyl acetylacetonate, and by incorporation of vanadium in the synthesis process. The prepared catalysts achieved a different distribution of vanadium species (isolated monomeric units with tetrahedral coordination, oligomeric units connected by V–O–V bonds up to distorted tetrahedral coordination, two-dimensional polymeric units in octahedral coordination, and bulk vanadium oxides). The contribution deals with the understanding of the relationship between the distribution of vanadium species and their activity in ODH of ethane. It has been found that both monomeric and oligomeric vanadium species play important role in ODH of ethane. The activity correlated with the population of oligomeric tetrahedrally coordinated vanadium species, which were evidenced by the UV–vis band at 315 nm. To analyze this effect, V-HMS catalysts were characterized by means of UV–vis spectroscopy, H<sub>2</sub>-TPR and N<sub>2</sub>-adsorption.

© 2008 Published by Elsevier B.V.

## 1. Introduction

Ethene is a very important industrial component. The main sources of ethene are steam cracking, fluid-catalytic cracking and catalytic dehydrogenation. These processes require high-energy input due to its endothermic character, and often catalysts regeneration due to a coke formation. Thus, the attention is currently focused to oxidative dehydrogenation (ODH) of ethane. In spite of intensive research, a low yield and selectivity to ethene still prevent its industrial application. Most catalytic systems reported in a recent review give the ethene yield below 20% [1]. On the other hand, many superior catalytic systems, such as Sr<sub>1.0</sub>La<sub>1.0</sub>Nd<sub>1.0</sub>O<sub>x</sub> [2], achieving the ethene yield approximately 40% have been reported [1].

Vanadium-based catalytic system represents one of the most studied catalysts in ODH of ethane and propane [1,3,4]. It has been recently reported that vanadium-based mesoporous silica materials of M41S family are active catalysts in ODH of propane (V-MCM-41 [5,6], V-MCM-48 [6], V-SBA-15 [7], and V-HMS [8]) and ethane (V-MCM-41 [5]). There have been also reported other vanadium-based catalysts such as V-alumina [9] and V-mesoporous alumina [10] active in ODH of ethane. Nevertheless, a lack of information is

on the relationship between the structure of vanadium species and their activity/selectivity.

The major factors affecting the ethene as well as propene formation and selectivity were reported to be the vanadium content [3,11], the vanadium surface density, the nature of the support and the reaction temperature [12]. It has been reported that dispersion of vanadium species up to vanadium loading as high as possible is a desirable to obtain an active and selective vanadium-based catalysts in ODH of light alkanes [8,13]. Banares and co-workers [9] reported that isolated and polymeric vanadium species possess the same TOF value for ethane activation. Activity of V-catalysts has been also attributed to the presence of V<sup>4+</sup> species, involved in the ODH reaction through a redox cycle [14,15]. It has been accepted that structural, textural and acidic/basic properties play important roles in the activity of mesoporous materials in ODH. Mesoporous molecular sieves of the M41S family, firstly reported in 1992 [16], have several advantages, such as high surface area and a very narrow pore size distribution in the mesoporous range.

Previously, we focused on the potential activity of V-HMS, V-MCM-41 and V-SBA-15 catalysts in ODH of ethane and to the role of reaction conditions on the activity/selectivity [17]. In this work we attempt to contribute to the understanding the active vanadium species in ODH of ethane. V-HMS catalysts were prepared by different methods achieving a different distribution of vanadium species, and compared in their catalytic activity.

<sup>\*</sup> Corresponding author. Tel.: +420 466 037 053.  
E-mail address: [libor.capek@upce.cz](mailto:libor.capek@upce.cz) (L. Čapek).

**Table 1**  
Characteristics of V-HMS-impr and V-HMS-synt catalysts

Catalyst	wt.% V	$S_{\text{BET}}$ (m <sup>2</sup> g <sup>−1</sup> )	V (nm <sup>−2</sup> )
HMS	0.0	835	0
V-HMS-impr	0.3	830	0.04
V-HMS-impr	1.3	810	0.18
V-HMS-impr	1.9	790	0.27
V-HMS-impr	2.4	670	0.43
V-HMS-impr	2.9	646	0.53
V-HMS-impr	3.2	390	0.97
V-HMS-impr	4.5	394	1.34
V-HMS-impr	8.8	90	11.54
V-HMS-synt	0.7	803	0.10
V-HMS-synt	2.0	700	0.33
V-HMS-synt	2.7	611	0.56
V-HMS-synt	6.8	401	1.89
V-HMS-synt	7.8	493	1.88

## 2. Experimental

Hexagonal mesoporous silica (HMS) was synthesized according to the procedure reported by Tanev and Pinnavaia [18]. HMS (835 m<sup>2</sup> g<sup>−1</sup>) was prepared by dissolving 13.6 g dodecylamine (DDA, Aldrich) in the mixture of 144.6 ml ethanol and 200 ml re-distilled water (re-H<sub>2</sub>O). After stirring for 20 min, 56 ml of tetraethylorthosilicate (TEOS, Aldrich) in 81 ml ethanol was added drop-wise and stirred. The synthesis was performed at 70 °C for 18 h under static conditions. The solid product was filtered, washed with re-H<sub>2</sub>O and finally calcined in air at 450 °C for 8 h. Structure and crystallinity of synthesized mesoporous support was verified by X-ray diffraction and scanning electron microscopy [13]. V-HMS-impr catalysts (0.3–9 wt.% V, Table 1) were prepared by impregnating HMS with solution of vanadyl acetylacetonate in ethanol. After impregnation, the catalysts were filtered and dried at room temperature for 24 h. Calcination was carried out for 8 h at 600 °C in air. V-HMS-synt catalysts (0.3–9 wt.% V, Table 1) were prepared by the same procedure as pure HMS. Additionally, the solution of vanadyl acetylacetonate in ethanol was dropwise added to the synthetic gel.

UV–vis diffuse reflectance spectra were recorded using GBS CINTRA 303 spectrometer equipped with a diffuse reflectance attachment with a spectralon-coated integrating sphere against a spectralon reference. Granulated materials (0.25–0.50 mm) were dehydrated under oxygen stream at 450 °C for 1 h, cooled to 150 °C in oxygen and followed by their evacuation at 150 °C under vacuum of 0.1 Pa for 15 min [17]. H<sub>2</sub>-TPR profile was monitored with a heating rate 10 °C/min in the temperature range 20–1000 °C. Quartz microreactor was charged with 100 mg of a dry catalyst. The reduction gas contained 5 vol.% H<sub>2</sub> in nitrogen with total flow rate 25 ml min<sup>−1</sup> [19]. The N<sub>2</sub>-adsorption isotherms were obtained at −196 °C using the through-flow chromatographic method. The relative pressure of nitrogen was varied in the range of 0.01–0.30. The specific surface area ( $S_{\text{BET}}$ ) was determined by the fitting of the experimental data to the BET isotherm [17]. The surface vanadium density (VOx surface density, VOx nm<sup>−2</sup>) was calculated as  $(N_A(w_V/100)/M_V S_{\text{BET}}) \times 10^{-18}$ , where  $N_A$  is Avogadro constant,  $w_V$  mass fraction of vanadium in V-HMS (wt.%),  $M_V$  is

molecular weight of vanadium (50.94 g mol<sup>−1</sup>) and  $S_{\text{BET}}$  is the specific surface area of V-HMS (m<sup>2</sup> g<sup>−1</sup>).

The oxidative dehydrogenation of ethane was carried out in a quartz through-flow micro-reactor at 550 and 600 °C and atmospheric pressure. The reaction mixture consisted of 7.5 vol.% C<sub>2</sub>H<sub>6</sub>, 2.5 vol.% O<sub>2</sub> and a rest of He was kept at a total flow of 100 ml min<sup>−1</sup> (W/F 0.12 g<sub>cat</sub> s ml<sup>−1</sup>). The oxygen and ethane concentrations and W/F represent important variables affecting the catalysts activity in ODH. The used reaction conditions represent the optimum values for V-HMS catalysts [17]. Concentrations of CO<sub>2</sub>, CO, O<sub>2</sub>, and hydrocarbons were provided by an on-line connected gas chromatograph Shimadzu GC 17A [17].

## 3. Results and discussions

### 3.1. ODH of ethane over V-HMS-impr and V-HMS-synt

Ethene, CO, and CO<sub>2</sub> were the main products in ODH of ethane (Table 2). Only a trace concentration of CH<sub>4</sub> was detected as a cracking product. Other hydrocarbons or its derivatives was not detected. The contribution of homogeneous gas-phase reactions was not observed as resulted from the zero conversion of ethane and oxygen in an empty reactor.

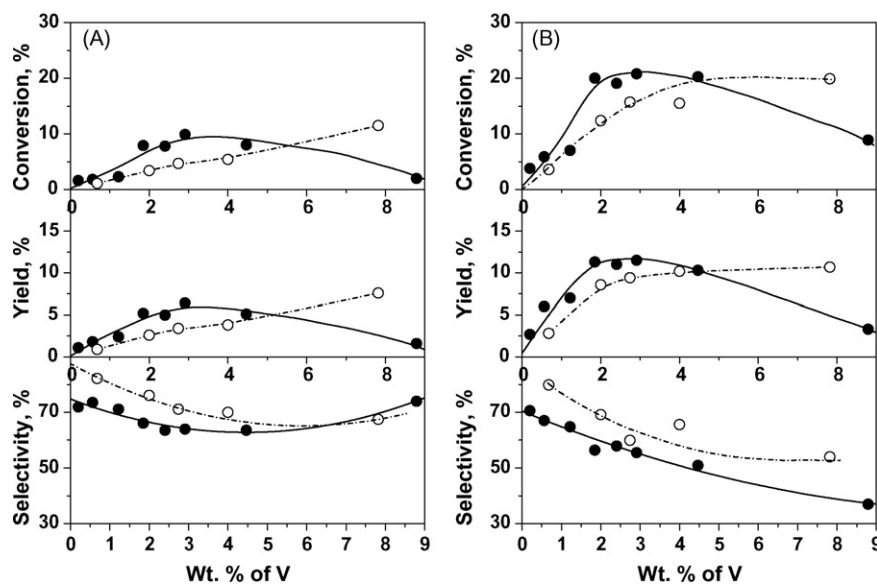
Fig. 1 shows the dependence of the ethane conversion, the ethene yield, and the selectivity to ethene on vanadium content in ODH of ethane over V-HMS-impr and V-HMS-synt catalysts at 550 and 600 °C. The activity of pure HMS was insignificant (the ethane conversion below 0.5%). The ethane conversion and the ethene yield increased with increasing vanadium content and with increasing temperature. The activity of V-HMS-impr and V-HMS-synt differs mainly in the maximum value of its activity. While V-HMS-impr catalysts achieved a maximum activity between 2 and 4.5 wt.% V, the activity of V-HMS-synt was shifted to higher vanadium content (the maximum was not achieved up to 8 wt.% V). Below 4.5 wt.% V, V-HMS-impr catalysts were more active in comparison with V-HMS-synt. The ethane conversion 22%, the ethene yield 12%, and the selectivity to ethene 55% was achieved with the most active V-HMS-impr containing 2.9 wt.% V at 600 °C. These values were comparable with that reported for V-mesoporous alumina [10] and V-MCM-41 [5,20].

Fig. 2 shows the selectivity-conversion behavior of V-HMS-impr and V-HMS-synt catalysts shown at Fig. 1. The selectivity to ethene decreased with increasing conversion (temperature, vanadium content). Solid line represents the selectivity-conversion behavior of V-HMS-impr catalysts with 0.3–4.5 wt.% V tested at 550 and 600 °C. This selectivity-conversion dependence correlated with that previously reported for V-HMS-impr with 2.4 wt.% V tested under varying reaction conditions (ethane and oxygen concentration and contact time) [17]. This indicates that the selectivity-conversion behavior would not be changed by either vanadium content or reaction condition. The selectivity-conversion behavior would be changed only by the preparation of vanadium-based catalysts. Dashed line represents the selectivity-conversion behavior of V-HMS-synt catalysts with 0.7–7.8 wt.% tested at 550 and 600 °C. V-HMS-synt materials did not exhibit such explicit selectivity-conversion dependence as V-HMS-impr. Although, V-HMS-synt catalysts (Fig. 2-dashed line) were slightly

**Table 2**  
Activity of V-HMS-impr and V-HMS-synt catalysts containing the similar vanadium content in ODH of ethane at iso-conversion conditions and 600 °C

Catalyst (wt.% V)	X(C <sub>2</sub> H <sub>6</sub> ) (%)	X(O <sub>2</sub> ) (%)	Y(C <sub>2</sub> H <sub>4</sub> ) (%)	S(C <sub>2</sub> H <sub>4</sub> ) (%)	S(CO) (%)	S(CO <sub>2</sub> ) (%)	Productivity (g(C <sub>2</sub> H <sub>4</sub> )/g <sub>cat</sub> h <sup>−1</sup> )	TOF (h <sup>−1</sup> )
V-HMS-impr (1.9)	11.8	56.8	7.5	63.4	29.2	7.1	0.39	59.5
V-HMS-synt (2.0)	12.4	54.1	8.6	69.2	22.1	8.3	0.22	26.1

Gas composition 7.5% ethane, 2.5% O<sub>2</sub> and He, 200 mg V-HMS-synt catalyst or 100 mg V-HMS-impr catalyst, total flow 100 ml min<sup>−1</sup>.



**Fig. 1.** Dependence of ethane conversion, ethene yield and selectivity to ethene on vanadium content in ODH of ethane over V-HMS-impr (●, —) and V-HMS-synt (○, - - -) at (A) 550 and (B) 600 °C. Gas composition 7.5% ethane, 2.5% O<sub>2</sub> and He, 200 mg catalysts, total flow 100 ml min<sup>-1</sup>.

more selective in comparison with V-HMS-impr, the difference was not significant. V-HMS-impr with 8.8 wt.% V exhibited a low ethane conversion as well as a low selectivity to ethene due to a presence of bulk vanadium oxides. On the other hand, V-HMS-synt with 7.8 wt.% V did not decrease in the selectivity-conversion behavior as vanadium oxide like species were not present in the material (see below).

Table 2 compares the activity/selectivity of V-HMS-impr and V-HMS-synt catalysts with the same vanadium loading (ca. 2 wt.% V) at iso-conversion experiment (the ethane conversion ca. 12%). V-HMS-synt was slightly more selective than V-HMS-impr, which was in an agreement with the results given in Fig. 2. The activity of V-HMS-impr and V-HMS-synt was compared in its ethene productivity, and Turn-Over-Frequency (TOF, the average number of catalytic cycle at one average vanadium atom per time unit). V-HMS-impr was significantly more active than V-HMS-synt.

### 3.2. Characterization of the catalysts

Fig. 3 shows UV-vis spectra of dehydrated V-HMS-impr and V-HMS-synt catalysts. Very low intensive bands at 215, 258 and

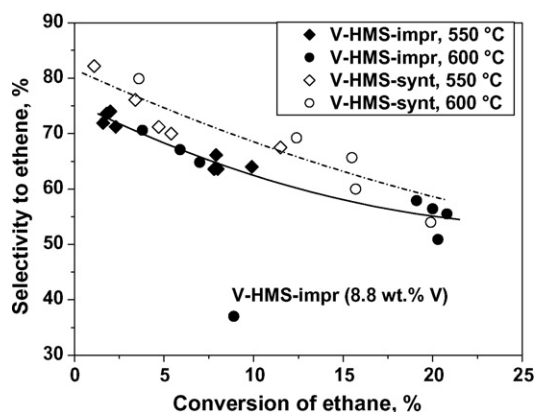


**Fig. 2.** Dependence of the selectivity to ethene on the ethane conversion obtained during ODH of ethane over V-HMS-impr (●, ◆) and V-HMS-synt (○, ◇). Gas composition 7.5% ethane, 2.5% O<sub>2</sub> and He, 200 mg catalysts, total flow 100 ml min<sup>-1</sup>, 550 (◆, ◇) and 600 (●, ○) °C.

300 nm were observed in the UV-vis spectra of pure HMS (Fig. 3A). Six bands with the maximum at approximately 215, 245, 275, 315, 395 and 490 nm were evidenced in the UV-vis spectra of dehydrated V-HMS-impr (Fig. 3A) and V-HMS-synt (Fig. 3B) catalysts after its deconvolution to Gaussian components. Firstly, UV-vis bands were formed at 215, 245 and 275 nm in the UV-vis spectra of V-HMS-impr and V-HMS-synt catalysts at low vanadium content. Secondly, the band was evidenced at 315 nm with increasing vanadium content. The intensity of the individual bands increased with increasing V content. The formation of the UV-vis band at 315 nm was shifted to higher vanadium content for V-HMS-synt in comparison with V-HMS-impr. Thirdly, a broad band at 395 nm was formed in V-HMS-impr and V-HMS-synt above 4.5 wt.% V. Finally, V-HMS-impr with 8.8 wt.% V exhibited a broad band at 490 nm. This band was not evidenced in the UV-vis spectra of V-HMS-synt catalysts even at the highest vanadium level. The UV-vis spectra of V-HMS-synt contained the bands at 215, 245, 275, 315 and low intensive band at 395 nm.

Vanadium-based catalysts are characterized by a lot of UV-vis bands. The UV-vis bands were reported to be at ca. 220, 275, 310, 359, 376, 468 and 538 nm for vanadium-based catalysts in a literature. The UV-vis band at 220 nm was attributed to (i) isolated tetrahedrally coordinated V<sup>5+</sup> species [21] and to (ii) the MCM-48 support [22]. The UV-vis bands at 240–250 [5,22–24], and 270 [23] nm were attributed to isolated monomeric tetrahedral vanadium species. However, the discrepancy is in the interpretation of the UV-vis bands at 300–320 nm and at 360–375 nm. The UV-vis band at 300–320 nm was attributed to (i) isolated monomeric tetrahedral vanadium species [22,24] and to (ii) oligomeric tetrahedral vanadium species [5,23]. The UV-vis band at 360–375 nm was attributed to (i) oligomeric tetrahedral vanadium species presenting V–O–V bridges [22,24], if the UV-vis band at 300–320 nm was attributed to isolated monomeric tetrahedral vanadium species and to (ii) octahedral coordinated V<sup>5+</sup> species [21,23], if the UV-vis band at 300–320 nm was attributed to oligomeric tetrahedral vanadium species. Thus, the UV-vis band corresponded to monomeric and oligomeric vanadium species are still under discussion. A broad band at 395 nm was attributed to aggregate vanadium entities in octahedral coordination [25]. The UV-vis bands at 468–490 [5,21] and 535 [21] nm were attributed to bulk vanadium oxides.

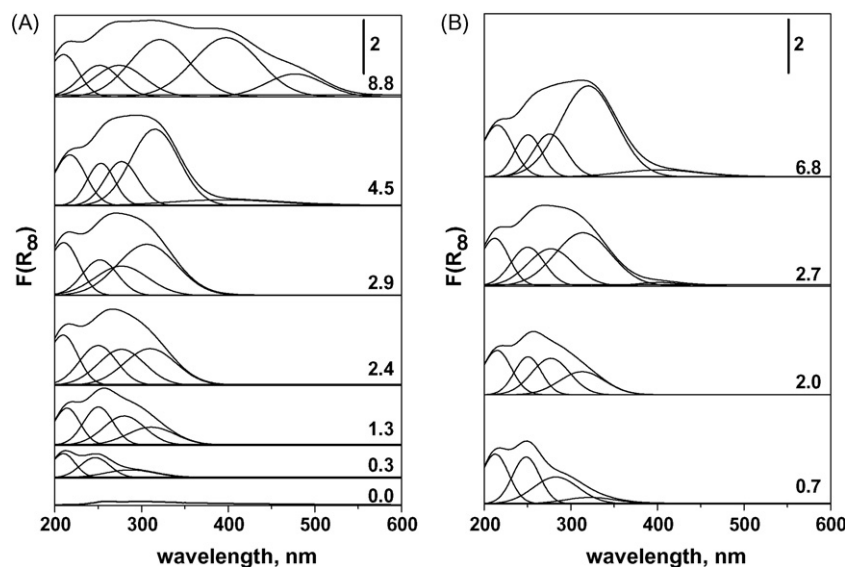


**Fig. 3.** Deconvoluted UV-vis spectra of dehydrated (A) HMS material and V-HMS-impr catalysts with 0.3, 1.3, 2.4, 2.9, 4.5 and 8.8 wt.% V and (B) V-HMS-synt catalysts with 0.7, 2.0, 2.7 and 6.8 wt.% V to Gaussian components.

Fig. 4 shows the dependence of relative intensity of individual UV-vis bands on vanadium content. While the relative intensity of UV-vis bands at 215, 245 and 275 nm decreased approximately all together with increasing vanadium content, relative intensity of the UV-vis band at 315 nm increased with increasing vanadium content. This change in the relative intensity was the same for V-HMS-impr and V-HMS-synt catalysts. Firstly, the UV-vis band at 215 nm would be assigned to isolated monomeric tetrahedrally coordinated  $V^{5+}$  species as (i) this band approximately follows the UV-vis bands at 245 and 275 nm, characteristic for isolated monomeric tetrahedrally coordinated  $V^{5+}$  species and (ii) this

intensive band was not observed in pure HMS material. This is in contrast with the results of Baltes et al. [22], who attributed the UV-vis band at 219 nm to MCM-48 support. Secondly, the UV-vis band at 315 nm would not reflect the same vanadium species as the UV-vis bands at 215, 245 and 275 nm due to its opposite dependence of the relative intensity on vanadium content shown in Fig. 4. Thus, the UV-vis band would be assigned to oligomeric tetrahedrally coordinated  $V^{5+}$  species.

Fig. 5 shows  $H_2$ -TPR profile of V-HMS-impr and V-HMS-synt catalysts.  $H_2$ -TPR profile of V-HMS-synt catalysts contained exclusive low temperature peak (568–590 °C) in the whole range of vanadium concentration (0.3–7.8 wt.% of V). The maximum of reduction peak slightly shifted from 568 to 590 °C with increasing vanadium content. On the other hand, the reduction bands at ca. 570 and 670–680 °C were included in  $H_2$ -TPR profile of all V-HMS-impr catalysts, even at low vanadium concentration.  $H_2$ -TPR profile of V-HMS-impr with 8.8 wt.% V contained the reduction band at 610 and 665 °C and a shoulder band at 715 °C. Thus, while V-HMS-synt catalysts were characterized by a narrow distribution of vanadium species, the distribution of vanadium species was different in the V-HMS-impr catalysts.

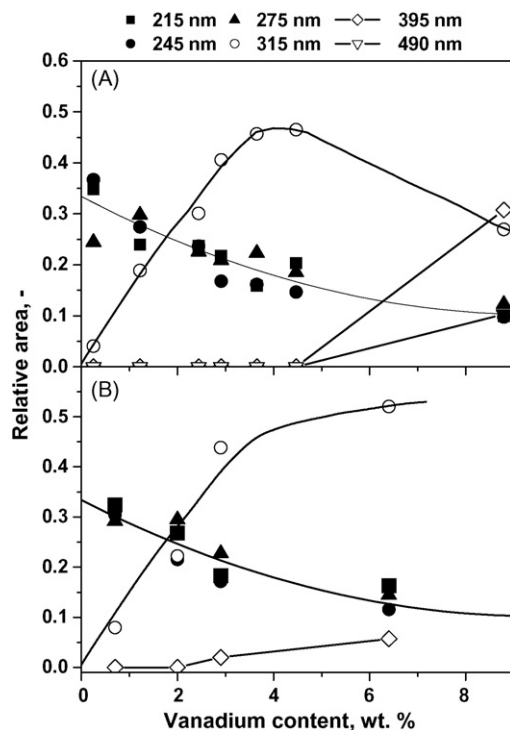


**Fig. 4.** Dependence of relative area of the individual UV-vis bands on wt.% of vanadium for (A) V-HMS-impr and (B) V-HMS-synt catalysts.

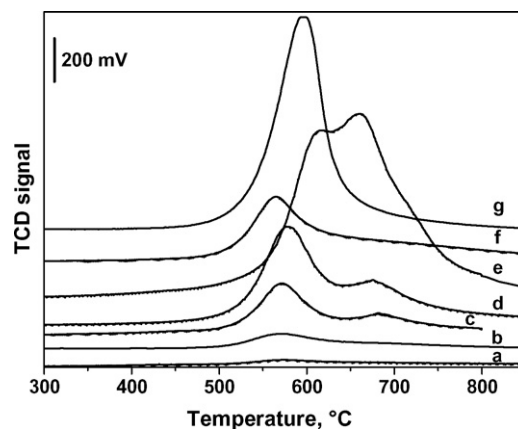


**Fig. 5.**  $H_2$ -TPR curves of chosen V-HMS-impr catalysts with 0.3 (a), 1.3 (b), 2.4 (c), 4.5 (d) and 8.8 (e) wt.% V, and V-HMS-synt catalysts with 2.0 (f) and 7.8 (g) wt.% V. Weight of the catalyst 100 mg.



Although V-HMS-synt and V-HMS-impr differ dramatically in their H<sub>2</sub>-TPR profiles (H<sub>2</sub>-TPR profile of V-HMS-synt catalysts contained exclusive low temperature peak at 568–590 °C in the whole range of vanadium concentration (0.3–7.8 wt.% of V), H<sub>2</sub>-TPR profile of V-HMS-impr catalysts contained two reduction bands at ca. 570 and ca. 670–680 °C up to 4.5 wt.% V), no dominant UV–vis band was observed in the UV–vis spectra of V-HMS-synt in contrast to V-HMS-impr. It is inconvenient to compare the reduction temperature with the reported data due its dependence on the reduction conditions (hydrogen partial pressure, heating rate), which differs in reported experimental data. However, it is generally accepted that the surface vanadium species would be reduced at lower temperature, whereas the oligomeric vanadium species or vanadium oxide-like species would be reduced at higher temperature [26–29]. Thus, there is not a simple correlation between the H<sub>2</sub>-TPR profile and the UV–vis spectra. The observation of one reduction peak and the UV–vis bands between 200 and 320 nm is in agreement with the results reported in literature [7]. The reduction peak at lower temperature (570 °C) should be related to the reduction of dispersed tetrahedral vanadium species. On the other hand, high temperature band at 680 °C represented only a part of oligomeric vanadium species detected by UV–vis band at 315 nm.

### 3.3. Relationship between the structure of vanadium species and its activity

The surface vanadium density (V/nm<sup>2</sup>) represents a parameter that allows comparing V-HMS catalysts in a wide range of vanadium concentration and specific surface area. A surface vanadium density increased with increasing vanadium content (Table 1) for V-HMS-impr and V-HMS-synt catalysts. The theoretical monovanadate monolayer was reported to be 2.3 V/nm<sup>2</sup> for TiO<sub>2</sub> [30] and Al<sub>2</sub>O<sub>3</sub>/SiO<sub>2</sub> [3], and ca. 0.7 V/nm<sup>2</sup> for SiO<sub>2</sub> [31]. Thus a surface vanadium density was below theoretical monovanadate monolayer up to 3 wt.% V (Table 1) for both V-HMS-impr and V-HMS-synt catalysts. V-HMS-impr with 3.2 and 4.5 wt.% V as well as V-HMS-synt with 6.8 and 7.8 wt.% have slightly higher value of surface vanadium density (Table 1) than that corresponded to theoretical monovanadate monolayer (0.7 V/nm<sup>2</sup> for SiO<sub>2</sub> [31]). On the other hand, V-HMS-impr with 8.8 wt.% of V (11.5 V/nm<sup>2</sup>) exhibited vanadium surface density above theoretical polyvanadate monolayer (7.5 V/nm<sup>2</sup> for Al<sub>2</sub>O<sub>3</sub>/SiO<sub>2</sub> [30]). Fig. 6 shows the dependence of the activity on a surface vanadium density. The activity increased with increasing vana-

dium surface density. While its maximum value was achieved between 0.3 and 1.3 V/nm<sup>2</sup> (2–4.5 wt.% V) for V-HMS-impr (V-HMS-impr with 8.8 wt.% V and 11.5 V/nm<sup>2</sup> had only low activity and selectivity), the activity increased with increasing vanadium surface density in the whole range of vanadium content for V-HMS-synt catalysts (up to 7.8 wt.%). At around 0.5 V/nm<sup>2</sup>, V-HMS-impr catalysts were much more active than V-HMS-synt catalysts. On the other hand, V-HMS-impr and V-HMS-synt had similar activity at around 1.5 V/nm<sup>2</sup>.

V-HMS-synt and V-HMS-impr catalysts differ in its activity and vanadium distribution. Isolated monomeric units with tetrahedral coordination, one-dimensional oligomeric units connected by V–O–V bonds up to distorted tetrahedral coordination, two-dimensional polymeric units in octahedral coordination and bulk vanadium oxides were observed in vanadium-based catalysts. While there was observed dramatic decrease of S<sub>BET</sub> for V-HMS-impr with 8.8 wt.% V (Table 1), there was observed low decrease of S<sub>BET</sub> corresponding to approximately 40% of its original value for V-HMS-synt with 7.8 wt.% V. According to H<sub>2</sub>-TPR profile, V-HMS-synt contained mainly vanadium species with its very narrow distribution (one reduction peak), whereas V-HMS-impr contained vanadium species with its more broad distribution. Thus, introduction of vanadium during of synthesis process prevent partial destruction of the mesoporous structure and it led to more efficient dispersion of vanadium preventing formation of vanadium oxide species. In literature, there was reported dramatic decrease of S<sub>BET</sub> for highly loaded V-based mesoporous materials (similar to that reported here for low active V-HMS-impr with 8.8 wt.% V) to 50–100 m<sup>2</sup> g<sup>−1</sup> [5] as well as (ii) low decrease of S<sub>BET</sub> corresponding to approximately 40% of its original value even above 7 wt.% V [7] (similar to that reported here for active V-HMS-synt with 7.8 wt.% V).

For V-HMS impr catalysts, the activity increased with increasing vanadium content and the maximum was achieved between 2 and 4.5 wt.% V. Than the activity decreased with increasing vanadium loading (Fig. 1). Decrease in the activity corresponded to the beginning of polymeric vanadium species and even bulk vanadium oxides formation (Fig. 3). V-HMS-impr with 8.8 wt.% had (i) UV–vis band at 490 nm (bulk vanadium oxide, Fig. 3), (ii) the reduction peak with a maximum at 610 and 715 °C (Fig. 5), (iii) a very low value of S<sub>BET</sub> (Table 1), and (iv) vanadium surface density above theoretical polyvanadate monolayer (Table 1). Decrease in the activity was also connected with decrease in the selectivity to ethene (Fig. 2). A dramatic decrease in the selectivity to ethene can be explained by the change in vanadium species distribution. While isolated vanadium species were predominately formed up to 4.5 wt.% V, polymeric species and finally bulk vanadium oxides were prevalent above 4.5 wt.%. Such species are responsible for the over oxidation of ethane and ethene to carbon oxides. On the other hand, bulk vanadium oxide was not evidenced in V-HMS-synt even at high vanadium concentration (Fig. 3). V-HMS-synt with 6.8 and 7.8 wt.% V had (i) much lower decrease in S<sub>BET</sub> (Table 1), and (ii) higher activity (Fig. 1) in contrast to V-HMS-impr with 8.8 wt.% V. It supports the already reported conclusion that dispersion of vanadium species up to vanadium loading as high as possible is desirable to obtain active and selective vanadium-based catalysts [13].

While there was clearly shown that two-dimensional polymeric units in octahedral coordination and bulk vanadium oxides had low activity and selectivity in ODH of ethane, it was hard to distinguish between the activities of monomeric and oligomeric vanadium species present in V-HMS catalysts. There was not found any clear and simple dependence of TOF on vanadium content in ODH of ethane, which indicated that more species were involved in the reaction. Nevertheless, the activity of V-HMS-impr and V-HMS-

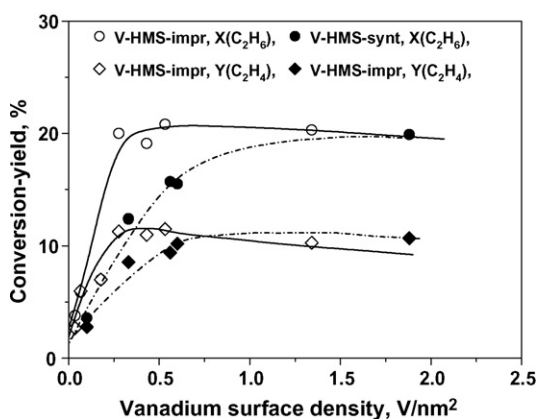


Fig. 6. Dependence of the ethane conversion (○, ●) and the ethene yield (◇, ◆) on vanadium surface density in ODH of ethane over V-HMS-impr (○, ◇) and V-HMS-synt (●, ◆) catalysts. Gas composition 7.5% ethane, 2.5% O<sub>2</sub> and He, 200 mg catalysts, total flow 100 ml min<sup>−1</sup>, 600 °C.

synt correlated with the increase in relative area of the UV–vis band at 315 nm (Figs. 3 and 4). The activity of V-HMS-synt was shifted to higher vanadium content in contrast to V-HMS-impr (Fig. 1) and surface vanadium density (Fig. 6) in comparison with V-HMS-impr. This also correlated with the low shift in relative area of the UV–vis band at 315 nm for V-HMS-synt to higher vanadium content (Fig. 4). The band at 315 nm was attributed here to oligomeric vanadium species. On the other hand, it is hard to suppose that only oligomeric vanadium species, represented by the UV–vis band at 315 nm, were the active sites in ODH of ethane.

Previously we reported that vanadium species present in V-HMS-synt catalysts are more active and effective in ODH of propane than that ones present in V-HMS-impr [32]. Moreover, the isolated monomeric vanadium units were supposed to be active and selective species for the ODH of propane [13,32]. In contrast to ODH of propane, V-HMS-impr catalysts were more active in ODH of ethane at 550 and 600 °C in comparison with V-HMS-synt catalysts (Fig. 1, Table 2). Thus, the different type of active species would be expected in ODH of ethane and propane. V-HMS-impr and V-HMS-synt catalysts differ in: (i) higher ethane ODH activity was observed for V-HMS-impr than for V-HMS-synt below 4.5 wt.% V (Fig. 1), (ii) there was observed the same maximum ethane ODH activity for V-HMS-impr and V-HMS-synt catalysts, which was achieved at different vanadium loading; the ethane conversion 22% and the ethene yield 12% was achieved for V-HMS-impr with 2.5–4.5% V, the ethene conversion 20% and the ethene yield 11% was achieved for V-HMS-synt with 7.8% V, and (iii) V-HMS-impr catalysts were more active at the same surface vanadium density at around 0.5 V/nm<sup>2</sup> in comparison with V-HMS-synt. The exclusive presence of low reduction peak at 570 °C was desirable in ODH of propane [32], but not for ODH of ethane (Table 2). These entire phenomenon indicate that ODH of ethane require both monomeric and oligomeric vanadium species. Monomeric vanadium species are slightly more selective (Fig. 2, Table 2), but oligomeric vanadium species are much more active in ODH of ethane (Table 2).

#### 4. Conclusions

V-HMS catalysts were prepared by impregnation with solution of vanadyl acetylacetonate (V-HMS-impr), and by incorporation of vanadium in the synthesis process (V-HMS-synt). The prepared catalysts achieved a different distribution of vanadium species (isolated monomeric units with tetrahedral coordination, oligomeric units connected by V–O–V bonds up to distorted tetrahedral coordination, two-dimensional polymeric units in octahedral coordination, and bulk vanadium oxides).

Polymeric vanadium species and even bulk vanadium oxides formation led to a dramatic decrease of  $S_{\text{BET}}$  and the activity. These species were formed at V-HMS-impr above 4.5 wt.% V, and not in V-HMS-synt even at high vanadium loading (6.8 and 7.8 wt.% V). The absence of vanadium oxide species also preserves the high  $S_{\text{BET}}$  for V-HMS-synt catalysts in comparison with V-HMS-impr.

Isolated monomeric vanadium species in tetrahedral coordination and oligomeric tetrahedrally coordinated vanadium species were present in the active V-HMS-impr and V-HMS-synt catalysts. The UV–vis bands at 215, 245 and 275 nm evidenced isolated monomeric vanadium species in tetrahedral coordination. The UV–vis band at 315 nm was attributed to oligomeric tetrahedrally coordinated vanadium species. While V-HMS-synt contained exclusive low temperature peak (568–590 °C) in the whole range

of vanadium concentration (0.3–7.8 wt.% of V), two reduction peaks at ca. 570 and 670–680 °C were included in H<sub>2</sub>-TPR profile of active V-HMS-impr catalysts up to 4.5 wt.% V. It was suggested that, the reduction peak at lower temperature (570 °C) should be related to the reduction of dispersed tetrahedral vanadium species, while the high temperature band at 680 °C represent only a part of oligomeric vanadium species detected by UV–vis band at 315 nm. The activity of V-HMS-impr and V-HMS-synt catalysts correlated with the population of oligomeric tetrahedrally coordinated vanadium species, which were evidenced by the UV–vis band at 315 nm.

While isolated monomeric tetrahedrally coordinated vanadium species were reported to be active and selective species in ODH of propane, oligomeric tetrahedrally coordinated vanadium species were suggested to be more active in ODH of ethane.

#### Acknowledgements

The authors gratefully thank to the Grant Agency of Czech Republic for financial support (projects No. 104/07/P038) and Ministry of Education, Youth and Sports (MSM0021627501). J. Adam also acknowledges support from the Grant Agency of the Czech Republic by the project 203/08/H032.

#### References

- [1] F. Cavani, N. Ballarini, A. Cericola, Catal. Today 127 (2007) 113.
- [2] S.A.R. Mulla, O.V. Buyevskaya, M. Baerns, Appl. Catal. A 226 (2002) 73.
- [3] A. Khodakov, B. Olthof, A.T. Bell, E. Iglesia, J. Catal. 181 (1999) 205.
- [4] A. Corma, J.M. López Nieto, M. Paredes, J. Catal. 144 (1993) 425.
- [5] B. Solsona, T. Blasco, J.M. López Nieto, M.L. Peña, F. Rey, A. Vidal-Moya, J. Catal. 203 (2001) 443.
- [6] M.L. Peña, A. Dejoz, V. Fornés, F. Reya, M.I. Vázquez, J.M. López Nieto, Appl. Catal. A 209 (2001) 155.
- [7] Y.M. Liu, Y. Cao, N. Yi, W.L. Feng, W.L. Dai, S.R. Yan, H.Y. He, K.N. Fan, J. Catal. 224 (2004) 417.
- [8] R. Zhou, Y. Cao, S.R. Yan, J.F. Deng, Y.Y. Liao, B.F. Hong, Catal. Lett. 75 (2001) 107.
- [9] M.V. Martínez-Huerta, X. Gao, H. Tian, I.E. Wachs, J.L.G. Fierro, M.A. Banares, Catal. Today 118 (2006) 279.
- [10] B. Solsona, A. Dejoz, T. García, P. Concepción, J.M. Lopez Nieto, M.I. Vázquez, M.T. Navarro, Catal. Today 117 (2006) 228.
- [11] M. Puglisi, F. Arena, F. Frusteri, V. Sokolovskii, A. Parmaliana, Catal. Lett. 41 (1996) 41.
- [12] T. Blasco, J.M. Lopez Nieto, Appl. Catal. A 157 (1997) 117.
- [13] P. Knotek, L. Čapek, R. Bulánek, J. Adam, Top. Catal. 45 (2006) 51.
- [14] M.P. Casaletto, L. Lisi, G. Mottogno, P. Patrono, G. Ruoppolo, G. Russo, Appl. Catal. A 226 (2002) 41.
- [15] F. Klose, T. Wolff, H. Lorenz, A. Seidel-Morgenstern, Y. Suchorski, M. Piórkowska, H. Weiss, J. Catal. 247 (2007) 176.
- [16] C.T. Kresge, M.E. Leonowicz, W.J. Roth, J.C. Vartuli, J.S. Beck, Nature 359 (1992) 710.
- [17] L. Čapek, J. Adam, T. Grygar, R. Bulánek, L. Vradman, G. Košová-Kučerová, P. Čičmanec, P. Knotek, Appl. Catal. A 342 (2008) 99.
- [18] P.T. Tanev, T.J. Pinnavaia, Science 267 (1995) 865.
- [19] R. Bulánek, B. Wichterlová, Z. Sobalík, J. Tichý, Appl. Catal. B 31 (2001) 13.
- [20] Q. Zhang, Y. Wang, Y. Ohishi, T. Shishido, K. Takehira, J. Catal. 202 (2001) 308.
- [21] E.V. Kondratenko, M. Baerns, Appl. Catal. A 222 (2001) 133.
- [22] M. Balthes, K. Cassiers, P. Van der Voort, B.M. Weckhuysen, R.A. Schoonheydt, E.F. Vansant, J. Catal. 197 (2001) 160.
- [23] V. Fornés, C. López, H.H. López, A. Martínez, Appl. Catal. A 249 (2003) 345.
- [24] H. Berndt, A. Martin, A. Brückner, E. Schreiber, D. Müller, H. Kosslick, G.-U. Wolf, B. Lücke, J. Catal. 191 (2000) 384.
- [25] P.R. Hari Prasad Rao, A.V. Ramasswamy, P. Ratnasamy, J. Catal. 137 (1992) 225.
- [26] M.M. Koranne, J.G. Goodwin, G. Marcelin, J. Catal. 148 (1994) 369.
- [27] H. Berndt, A. Martin, A. Brückner, E. Schreiber, D. Müller, H. Kosslick, G.U. Wolf, B. Lucke, J. Catal. 191 (2000) 384.
- [28] J. Keranen, A. Auroux, S. Ek, L. Niinisto, Appl. Catal. A 228 (2002) 213.
- [29] E.P. Reddy, R.S. Varma, J. Catal. 221 (2004) 93.
- [30] G. Centi, Appl. Catal. A 147 (1996) 267.
- [31] I.E. Wachs, B.M. Weckhuysen, Appl. Catal. A 157 (1997) 67.
- [32] R. Bulánek, H. Sheng-Yang, P. Knotek, L. Čapek, in preparation.